

Proceedings of

12th Structural Engineering Convention - An International Event (SEC 2022)



Effect of Debonding on Axial Response of Concrete Filled Steel Tubular Columns

Manigandan R^{1,*}, Manoj kumar²

Department of Civil Engineering, Research Scholar, Birla Institute of Science and Technology, Rajasthan, 333 031, India ² Department of Civil Engineering, Associate Professor, Birla Institute of Science and Technology, Rajasthan, 333 031, India

Paper ID - 010389

Abstract

The axial strength and ductility of concrete filled steel tubes is significantly improved due to two major factors namely, firstly due to confining effect provided by steel tube, and secondly due to the synergistic interaction between steel tube & concrete core. Sometimes, the contact between concrete core and steel tube is vanished and debonding between concrete core and steel tube (normal referred as gap) occurs owing to various reasons such as improper compaction, shrinkage in concrete, lack of curing of encased concrete, and due to non-uniform distribution of load at column top. Due to occurrence of gap, the composite action between concrete core and steel tube no longer remains effective the concrete core becomes unconfined in the initial phase of loading, consequently, the axial load carrying capacity of the concrete filled steel tubular (CFST) column decreases. The aim of this paper is to numerically investigate the effect of the gap between concrete core and steel tube on the axial load-deformation response and to Comparisons the predicted column strengths according to the Eurocode-4. In the present study, the gap between square section concrete core and encasing steel tube is considered on all the four sides with the magnitude of gap as 1 mm and 2 mm. Moreover, in order to investigate the effect of the gap on different size of square section CFST columns, keeping the length of column and steel tube thickness as constant 540 mm and 3.8 mm respectively, the side length of square section CFST column has been varied between 140 mm to 200 mm at an interval of 20 mm. The nonlinear finite element analysis of the CFST columns has been performed using the Abaqus where the C3D8R element has been used to discretize the concrete core as well as steel tube and the Drucker-Prager model has been used to simulate plastic behaviour of concrete. It has been observed that the presence of gaps between concrete core and steel tube significantly reduces the axial strength square CFST column.

Keywords: CFST, square section, gap, Abaqus, axial load-deformation, Drucker-Prager model

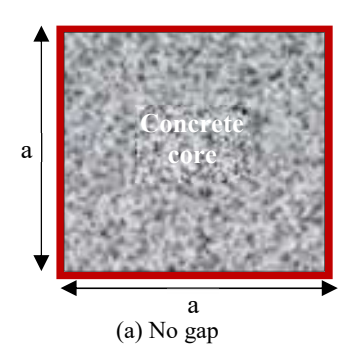
1. Introduction

In recent eras the use of concrete filled steel tubular (CFST) columns in structural applications is rapidly growing due to enhanced strength, high ductility, and large energy absorption capacity [1]. The improved structural performance of CFST columns is attributed mainly because of two reasons, firstly the composite action between concrete core and steel tube, and secondly the confining effect provided by steel tube. The adequate composite action between concrete core and steel tube necessitates the synergistic interaction between the outer surface of concrete core and the inner surface of steel tube [2,3]. In the CFST columns, having no gap between concrete core and steel, the adhesion between the steel tube and the concrete core develops initial bond and it is termed as chemical bond. The chemical bond is an elastic brittle shear transfer mechanism and remains active only in early stage of loading until the shear stress at interface remains less than the shear resistance due to chemical bond. Once the interface

In the circular section CFST columns, the gap may be of two types namely a uniform gap along the periphery of concrete core, normally referred as circumferential gap, and a non-uniform gap around the concrete core is called shear stress exceeds the chemical bond shear strength, chemical bond is broken, and this phenomenon is referred as debonding. After the debonding initiation, the shear resistance at interface is governed by two features namely mechanical micro-locking between concrete core & steel tube, and the frictional resistance that depends on the interface pressure and the coefficient of friction. In the analysis of CFST columns, normally it is assumed that there exists a perfect interaction between steel tube and concrete core, however, it remains of significant concern owing to improper compaction, shrinkage in concrete, lack of curing of encased concrete, temperature effects, and due to nonuniform distribution of load at column top. The imperfect interaction between the constituent materials of CFST, causes gap between concrete core and steel tube, as a result, the concrete core becomes unconfined and the axial strength of CFST column decreases.

spherical gap [3]. However, in square section CFST columns, gaps may be of along the all the four sides of square section concrete core, as shown in Fig 1.

*Corresponding author. Tel: +919789801266; E-mail address: rmani3830@gmail.com



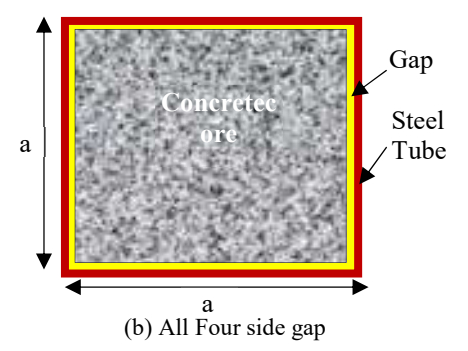


Fig. 1 Square CFST column of cross-section with and without Gap

The structural response of CFST column is complex owing to the nonlinear material behaviour of concrete and steel, and also the non-linearity associated with friction between steel tube & concrete. Moreover, the complexity in the structural behaviour of CFST is further enhanced due to presence of gap between concrete core and steel tube, if any. In order to understand the axial load-deformation response of CFST columns, generally, tests are performed in the laboratory which portray the real behaviour of CFST columns. Few experimental studies have been made in the past to investigate the effect of gaps on the ultimate load-carrying capacity of circular section CFST columns [9 -11], however, no experimental study appears in the context of square section CFST columns with gaps. Liao [10 - 12], tested the circular section short columns with circumferential and spherical gaps and observed that the ultimate compressive strength of the CFST short column decreases by 23% and 29%, respectively for the gaps of magnitude 0.55% and 1.1% of the column diameter [3]. Xue et al. performed the experiments to examine the effect of debonding on the ultimate load capacity and ductility in terms of reduction coefficients. They observed that the coefficients for both axial load and ductility decrease with increase in debonding arc-length to perimeter ratio. Moreover, they noticed that in the post-peak regime, the axial load in circular CFST columns with gaps decreases much faster than that in circular CFST column without debonding.

With the advent of the computer, it is possible to simulate the experimentally observed structural performance of CFST columns by carrying out the nonlinear finite element analysis using proper modelling for materials behaviour and the interaction between steel tube and concrete core [4-6]. Liao et al. [10] simulated the experimentally observed behaviour of axially loaded circular section CFST columns with circumferential gaps [8] and observed that the numerically determined ultimate strengths of CFST columns were close to those obtained experimentally and the difference in strengths were 1.82% and 4.82% for 1 mm and 2 mm gaps respectively. Han [11] compared the numerically determined collapse load of eccentrically loaded circular section CFST columns with circumferential gaps and concluded that the experimentally obtained structural response of eccentrically loaded CFST column may satisfactorily be predicted using the non-linear finite element analysis. The published literature revels that no study has been performed to assess the effect of gap on structural response of square section CFST columns.

The aim of this paper is to employ the nonlinear finite element program ABAQUS [10] to numerically evaluate the impact of the gap between square concrete core and encased steel tube on the axial load-deformation response of section CFST columns. In this study, the plastic behaviour of concrete has been modelled using the Drucker-Prager (D-P) model available in Abaqus [10], and a five-stage stress-strain relation has been assumed to model the steel tube. For the validation of adopted materials modelling and mesh size, the finite element results for the CFST columns with no-gap are compared for circular as well as square sections. To validate the finite element modelling for CFST columns with gap, the circular sections are considered, since no experimental data are available for the square section CFST with the gap. Finally, to investigate the effect of gaps between steel tube and concrete core on the structural response of the square CFST, keeping the tube thickness and length constant, the side length of the square section is varied from 140 mm to 200 mm at an interval of 20 m and the gaps between the concrete core and steel tube are considered as 1 mm and 2 mm as shown in Fig. 1 (a & b), and the results are compared with CFST columns with no-gap.

2. Modeling of Material and Interaction

In order to predict the non-linear structural response of CFST columns via the finite element method using the Abaqus, it is essential to develop the stress-strain relationship for steel and concrete together with the modelling of the interaction between steel tube and concrete core [11]

2.1 Modeling of Steel Tube

The stress-strain curve was divided in to five stages. The elastic stage (O-A), elastoplastic stage (A-B), plastic stage (B-C), hardening stage (C-D), and the secondary plastic stage (D-E) as shown in Fig.2

$$\begin{split} \sigma &= E_s \varepsilon & for \ \varepsilon \leq \varepsilon_1 \ (=0.8 \text{fsy/Es}) \\ \sigma &= -A \varepsilon^2 + B \varepsilon + C & for \ \varepsilon_1 < \varepsilon \leq \varepsilon_2 \ (=1.5 \varepsilon_1) \\ \sigma &= f_{sy} & for \ \varepsilon_2 < \varepsilon \leq \varepsilon_3 (=10 \varepsilon_2) \\ \sigma &= f_{sy} \left[1 + 0.6 \frac{\varepsilon - \varepsilon_3}{\varepsilon_4 - \varepsilon_3} \right] & for \ \varepsilon_3 < \varepsilon \leq \varepsilon_4 (=100 \varepsilon_2) \\ \sigma &= 1.6 f_{sy} & for \ \varepsilon > \varepsilon_4 \end{split}$$

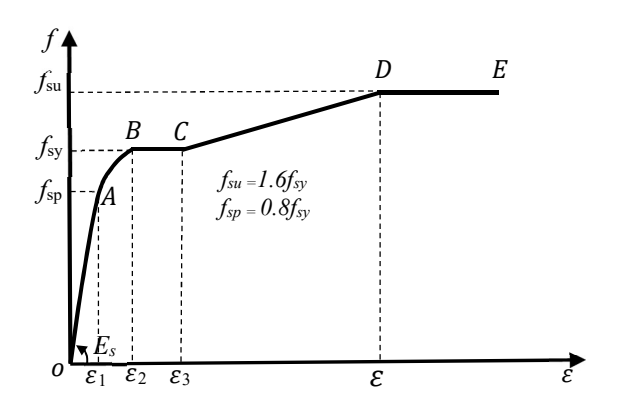


Fig. 2 Stress-strain curve for steel

Where,
$$A = \frac{0.2f_{sy}}{(\varepsilon_2 - \varepsilon_1)^2}$$
, $B = 2A\varepsilon_2$, $C = 0.8f_{sy} + A\varepsilon_1^2 -$

 $B\varepsilon_1$, and, E_s is the modulus of elasticity of steel. In the present study the modulus of elasticity of steel is considered as 2×10^5 N/mm² and the Poisson's ratio (μ_s) is taken as 0.3.

2.2 Modeling of Concrete Core

In the CFST columns, concrete is subjected to laterally confining pressure, as a result the uniaxial compressive strength and the corresponding strain are significantly enhanced. The enhanced compressive strength of concrete, f'_{cc} and the increased ultimate strain ε'_{cc} due to lateral confining pressure, f_1 are defined as

$$f'_{cc} = f_c + k_1 f_1$$

$$\varepsilon'_{cc} = \varepsilon'_c \left[1 + k_2 \frac{f_1}{f'_c} \right]$$

Where f_c' is the compressive strength of concrete in the unconfined state, ε_c' is the peak strain in unconfined concrete which is taken as 0.003 and the constants k_1 and k_2 are assumed as 4.1 and 20.5 respectively [16]. The lateral confining pressure, f_l for circular and square section CFST columns is calculated using following empirical equations [4].

For Circular Section

$$\frac{f_1}{f_y} = 0.043646 - 0.000832 \left[\frac{D}{t} \right] \qquad for \ 21.7 \le \frac{D}{t} \le 47$$

$$\frac{f_1}{f_y} = 0.006241 - 0.0000357 \left[\frac{D}{t} \right] \qquad for \ 47 \le \frac{D}{t} \le 150$$

For Square Section

$$\frac{f_1}{f_y} = 0.055048 - 0.001885 \left[\frac{a}{t} \right] \qquad for \ 17 \le \frac{a}{t} \le 29.2$$

$$\frac{f_1}{f_y} = 0 \qquad \qquad for \ 29.2 \le \frac{a}{t} \le 150$$

Where, f_y = yield strength of the steel tube, D = outer dimension of steel tube, a = side length of the CFST column section, and t = thickness of the steel tube.

The uniaxial stress-strain relationship for the confined concrete developed by Hu et al. [8] is a combination of parabolic segment (O to A) followed by a straight line (A to B) as shown in Fig.3. The stress-strain relation for parabolic segment is expressed as

$$f = \frac{E_{c}\varepsilon}{1 + (R + R_{E} - 2)\left[\frac{\varepsilon_{c}'}{\varepsilon_{cc}'}\right] - (2R - 1)\left[\frac{\varepsilon_{c}'}{\varepsilon_{cc}'}\right]^{2} + R\left[\frac{\varepsilon_{c}'}{\varepsilon_{cc}'}\right]^{2}}$$

where,
$$R = \frac{R_E(R_{\sigma}-1)}{(R_{\varepsilon}-1)^2} - \frac{1}{R_E}$$
; $R_E = \frac{E_c \, \varepsilon'_{cc}}{f'_{cc}}$; $R_{\varepsilon} = R_{\sigma} = 4$

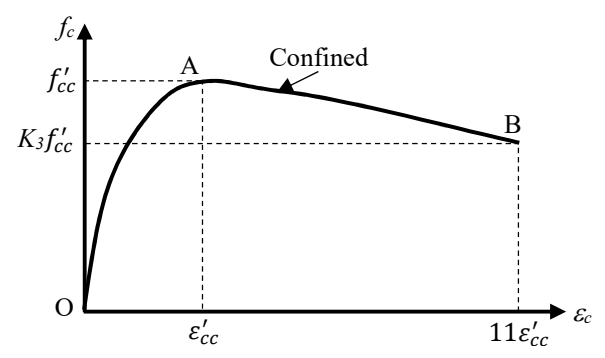


Fig. 3. Stress-Strain Curve of Confined

In the descending part of the curve (A to B) stress is assumed vary linearly up to the failure stage of concrete. The stress and strain at failure stage f_u and ε_u are assumed K_3f_c' and $11\varepsilon_c'$ respectively [17]. The value of K_3 for circular and square sections concrete filled steel tubes is calculated using following empirical equations:

For Circular Section

$$K_3 = 1$$
 for $21.7 \le \frac{D}{t} \le 40$
 $K_3 = 0.0000339 \left[\frac{D}{t}\right]^2 - 0.010085 \left[\frac{D}{t}\right] + 1.3491$ for $40 \le \frac{D}{t} \le 150$

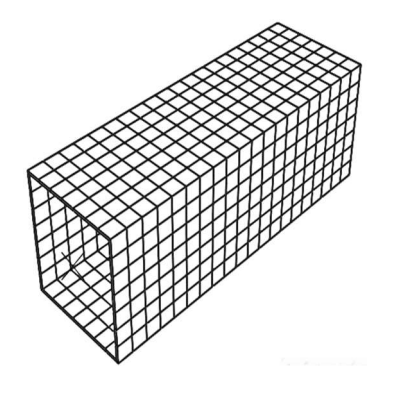
For Square Section

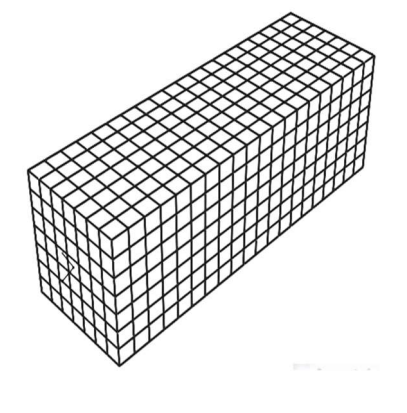
$$K_3 = 0.000178 \left[\frac{a}{t}\right]^2 - 0.02492 \left[\frac{a}{t}\right] + 1.2722$$
 for $17 \le \frac{a}{t} \le 70$
 $K_3 = 0.4$ for $70 \le \frac{a}{t} \le 150$

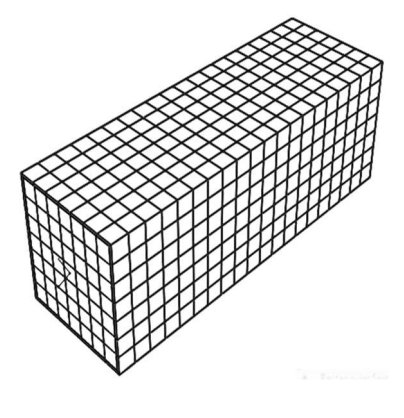
In the CFST columns containing gap between concrete core and steel tube, concrete core remains unconfined in the initial phase of loading, nevertheless, with increase in load on column, concrete expands laterally and for the gaps of magnitude less than 1 mm, concrete may re-interact with tube to initiate confining pressure [13]. This infers that for modelling the concrete encased in steel tubes with the initially assumed gaps of 1 mm and 2 mm gaps (≥ 1 mm), the unconfined stress-strain curve must be used. The Attard-Setunge's [23] uniaxial stress-strain model for unconfined concrete has been adopted in present study for modelling the concrete core.

In the Attard-Setunge's [23] model, stress-strain relationship for unconfined concrete consists of two segments, namely ascending part (from point A to B) and descending part (from point B to C) and for both the segments the variation of stress with strain is assumed parabolic. In this model, the stress-strain relationship for unconfined concrete is presented in the non-dimensional form where the stress and strain at any stage are normalized by strength of concrete f_c' and the strain at peak ε_c' . respectively. At any stage of loading, f and ε are the stress and strain in concrete, then the stress-strain relation for unconfined concrete in terms of non-dimensional parameters X (= $\varepsilon/\varepsilon_c'$) and $Y = f/f_c'$) is defined as

$$Y = \frac{AX + BX^2}{1 + CX + DX^2}$$







(a) Steel tube

(b) Concrete core

(c) Steel Tube plus concrete core

Fig. 4 Finite Element Model

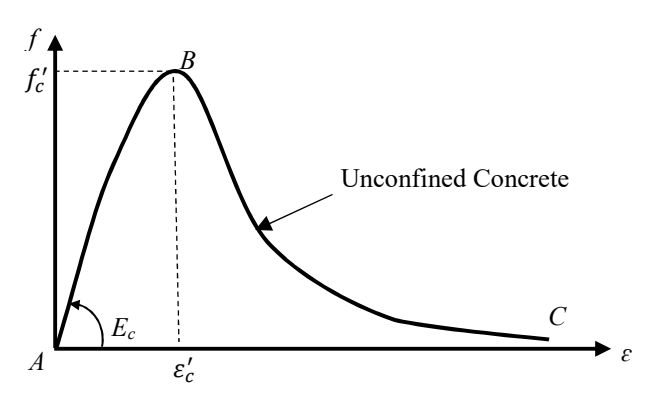


Fig. 5. Stress-strain curve for unconfined concrete

Where A, B, C, and D, are the parameters defining the stress-strain curve for unconfined concrete. For the ascending part of the curve (from A to B) the model parameters are

$$A = \frac{E_{ti}\varepsilon_0}{f_0}; B = \frac{(A-1)^2}{\alpha\left(1 - \frac{f_{pl}}{f_0}\right)} + \frac{A^2(1-\alpha)}{\alpha^2 \frac{f_{pl}}{f_0}\left(1 - \frac{f_{pl}}{f_0}\right)} - 1; C = (A-2);$$

$$D = (B+1)$$
Where, $\alpha = \frac{E_{ti}}{E_c}$, E_{ti} is the initial tangent modulus, E_c is the

secant modulus measured at a stress level f_{pl} , usually taken as 0.45f₀. The initial tangent modulus E_{ti}, is assumed to vary linearly between $1.17E_c$ and E_c for concrete strength 20 and 100 MPa respectively.

$$E_c = (3320\sqrt{f_c'} + 6900) \left(\frac{\rho}{2320}\right)^{1.5}$$

 $E_c = (3320\sqrt{f_c'} + 6900) \left(\frac{\rho}{2320}\right)^{1.5}$ Where, f_c' is the cylindrical strength of concrete and ρ is surface dry unit weight of concrete in kg/m³. Moreover, the strain at peak, ε'_c for the concrete produced with crushed aggregates is calculated as [23]

$$\varepsilon_c' = \frac{f_c'}{E_c} \frac{4.26}{4 \int f_c'}$$

For the descending part of the curve, the model parameters A through D are calculated as

$$A = \frac{f_{ic}}{\varepsilon'_c \varepsilon_{ic}} \frac{(\varepsilon_{ic} - \varepsilon'_c)^2}{f'_c - f_{ic}}; B = 0; C = A - 2; D = 1,$$
Where, $\frac{f_{ic}}{f'_c} = 1.41 - 0.17 \ln(f'_c)$ and $\frac{\varepsilon_{ic}}{\varepsilon'_c} = 2.5 - 0.3 \ln(f'_c)$

2.3 Modeling of Interaction Between Steel Tube and Concrete Core

In the CFST columns, concrete core is confined with steel tube as a result, in addition to confining pressure, there exist the bond as well as the frictional resistance at the interface. The shear resistance at interface is normally incorporated in analysis using the Coulomb's friction law. According to Coulomb's friction model, shear stress across the surfaces may be transmitted until the magnitude of shear stress at interface is greater than the limiting value τ_c . Once the relative slip is developed between the concrete core and steel tube then shear stress is assumed constant. The τ_c depends on the lateral confining stress p between concrete core and steel tube, and its magnitude is expressed as

$$\tau_c = \mu p \geq \tau_{bond}$$

Where, μ is the friction coefficient and its value is commonly considered as 0.6 in this study and τ_{bond} is average surface bond stress and for circular section CFST columns, it is determined as [25].

$$\tau_{bond} = \left[2.314 - 0.0195 \cdot \left(\frac{B}{t} \right) \right]$$

Where 'B' and 't' are the outer dimension and thickness of the steel tube, respectively. The bond strength of square section CFST column is taken as 0.75 times the bond strength of circular section.

3. Finite Element Discretization

The eight-node reduced integration based linear solid elements C3D8R having three translation degrees of freedom at each node is used for meshing the concrete core as well as the steel tube [3]. The number of elements in the concrete core along the length and the perimeter were kept equal to the number of elements used to discretize steel tube along the length and perimeter respectively to coincide the nodes of core and steel tube. To determine the optimum mesh size, a mesh sensitivity analysis was carried out. The mesh sensitivity study was revealed for square section CFST columns with no-gap, twenty elements along the length and

			steel CFST col.	Str. of Str. of Steel Con		Ultimate strength of CFST column (in kN) for								
Sec.		of of steel tube			Comp. Str. of Conc.	No-Gap		1 mm gap all around			2 mm gap all around			
shape						Exper. Abaq		qus	Exper.	Abaqus		Exper.	Abaqus	
					(MPa)		Pub.	Pres.	(Pub.	Pub.	Pres.	(Pub.	Pub. Liter.	Pres.
						Liter.)	Liter.	Study	Liter.)	Liter.	study	Liter.)	T do. Liter.	study
Cir.	180	3.80	540.0	360.0	51.28	2110 ^[11]	2100[8]	2100	1640 ^[11]	1610 ^[8]	1649	1440 ^[11]	1460 ^[8]	1461
Sq.	127	4.34	609.6	357.0	26.00	1106 ^[17]	1130 ^[4]	1128						

Table -1. Comparisons between Experimental and Finite Element simulation results to verify FE Model

seven elements along the side of the square section gives results closer to experimental data and the same number elements are used to discretize all the square section CFST columns (with and without gap) was taken in this study. A typical finite element mesh for the square CFST column is shown in Fig. 4 (a-c). For circular section columns with and without a gap, which were used for validation of finite element modeling, the column length was divided into 20 elements same as square and discretization the circumference into 20 elements was found adequate to produce the FEM results closer to experimental data.

3.1 Application of Load and Boundary Conditions

For the application of boundary conditions and axial load on the CFST column, the rigid body tie constraints were considered. At the top face of the column, a reference point (RP1) was assigned, and all the nodes at the top face of the column were connected to RP1 through rigid ties. At the top face of the column, the boundary conditions, as well as an axial load, was applied at RP1. In the similar way, the reference point RP2 was assigned at the bottom face of the column and the corresponding boundary condition to the bottom end of the column was applied at RP2. While determining the axial load carrying capacity of the column experimentally the column is generally supported on the rigid bottom plate, and the load is applied to the rigid plate placed at the top of the column in order to uniformly distribute the applied load over the entire cross-sectional area, i.e., steel tube as well as the concrete core. Since these plates are in

direct contact with the infilled concrete as well as the periphery of steel tube, the rotation and lateral translation of the column ends were restricted due to friction between rigid plates and concrete core & steel tube. In order to replicate the same boundary conditions, the bottom reference point RP2 was fully restrained (i.e., $u_x = v_y = w_z = \theta_x = \theta_y = \theta_z = 0$) while the top reference point RP1 was allowed to displace in the loading direction only ($u_x = v_y = \theta_x = \theta_y = \theta_z = 0$; $w_z \neq 0$) as shown in Fig 6. The load was applied at the top reference points RP1 in the form displacement-controlled load.

4. Verification of Numerical Modeling

In order to validate the material modelling and mesh size used in the present study, the finite element results obtained in the present study for circular and square section CFST columns are compared with the experimental data. The experimental data obtained by Liao [11] for circular section columns have been considered for validating the proposed modelling in simulating the axial load-deformation behaviour of CFST circular columns with and without the gap. For the square section CFST columns with gaps, no experimental data are available, therefore, experimental data obtained by Schneider [17] for the square section with no-gap only have been considered for validating the modelling of the CFST square section columns. Moreover, the results obtained in the present study have also been compared with the finite element results presented by Liao [8] and Hu et al. [4] for circular and square sections, respectively. The geometrical details and material properties of circular and square sections considered for validation purposes are shown in Table 1. For the simulation of plastic deformation in the concrete core, the

Drucker-Prager model has been used, and the parameters associated with this model given as input in Abaqus are: Angle of friction = 20° , Flow Stress ratio = 0.8; and Dilation angle = 20° . Comparisons between Experimental and Finite Element simulation results to verify FE Model

In the present study, the ultimate axial load carrying capacity and the axial load-deformation response of square section CFST columns with no-gap, and for the circular section CFST columns with- and with-out gap are compared together with the experimental data and numerical simulation results obtained by Liao [8] and Schneider [17]. Table 1 and Fig.7. show that the ultimate load-carrying capacity vs. the axial load-deformation response determined in the present study is in close agreement with the experimental data as well as the FEM results obtained in previous studies.

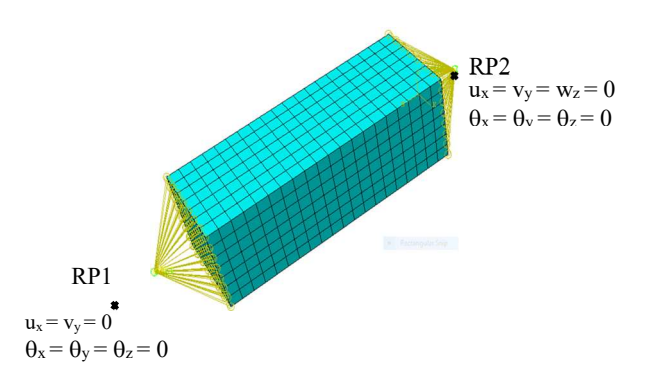
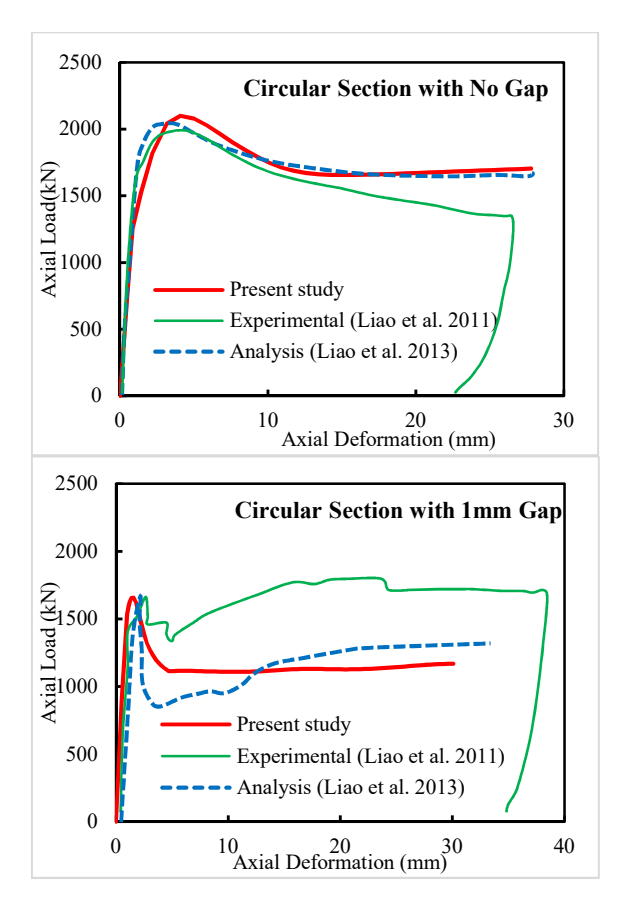


Fig. 6. Boundary condition with the reference point (RP1 and RP2)



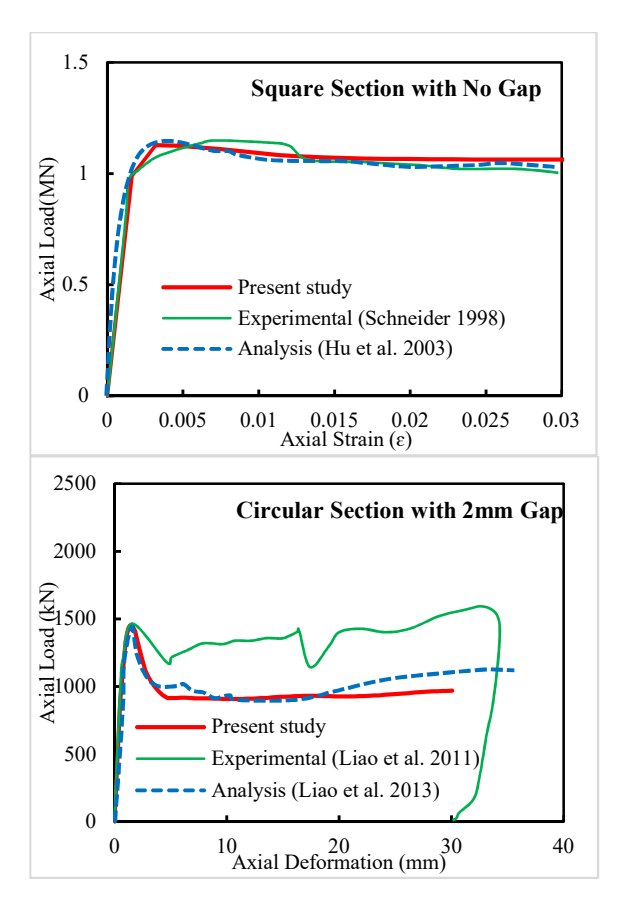


Fig.7 Validation of Numerical Model of Circular and Square Section columns with and without gap

Table-2. Effect of different Side Gaps on Ult. Str. of CFST Square Columns of various side lengths

G: 1 1 41 C	T. 1	(a/t)	CFST	Ultimate Load						
Side length of	Tube		Length	For gap	(g)=1 mm	For gap (g)=2 mm		P_{u,g_0}		
Sq.,section 'a' (mm)	Thick., t (mm)		L (mm)	P_{u,g_1} (kN)	$\left(\frac{P_{u,g_1}}{P_{u,g_0}}\right) \times 100$	P_{u,g_2} (kN)	$\left(\frac{P_{u,g_2}}{P_{u,g_0}}\right) \times 100$	(kN)		
140	3.8	36.8	540	1655	98.10	1636	96.98	1687		
160	3.8	42.1	540	2070	98.67	2038	97.14	2098		
180	3.8	47.4	540	2524	98.59	2501	97.70	2560		
200	3.8	52.6	540	3012	99.60	2980	98.54	3024		

5. Finite Element Modeling of Square Section CFST Column with Gap

In order to investigate the influence of the gap between the concrete core and steel tube on the axial load-deformation behaviour of CFST columns, the side length (a) of CFST column sections is varied between 140 mm to 200 mm at an interval of 20 mm. For all the cross-sectional dimensions considered, the CFST columns with no gap have been considered as the reference sections and to examine the effect of gaps, 1 mm and 2 mm gaps are considered on all four sides of the square section. The yield strength of steel tube and compressive strength of concrete have been kept constant for all the columns considered, and their values considered are 360 N/mm² and 51.28 N/mm², respectively. Moreover, the Poisson's ratio of concrete is taken as 0.2, and the modulus of elasticity is calculated from the compressive strength of

concrete as E_c = 4730 $\sqrt{f_c'}$, where f_c' is the cylindrical compressive strength of concrete.

6. Influence of Gap on Ultimate-Load Carrying Capacity of CFST Column

The ultimate load-carrying capacity of square section columns of different side-lengths for no-gap case $(P_{u,g0})$ together with the ultimate load-carrying capacity of the column corresponding to the gap of 1 mm $(P_{u,g1})$ and a gap of 2 mm $(P_{u,g2})$ on all four sides are summarized in the Table.2. For examining the effect of gaps on different sized columns, the $P_{u,g1}$, and $P_{u,g2}$ are normalized with respect to the ultimate load-carrying capacity of corresponding reference section $(P_{u,g0})$. The normalized load factor $[=(P_{u,g}/P_{u,g0})\times100]$ for various sized columns with for 1 mm and 2 mm gaps are shown in the Table.2, and the same are plotted in Fig.9. It may be observed from the table.2 that due to all four side gap

Side	Lateral Disp. at Mid-ht.	Gap (mm)	Lateral Disp. (mm) at mid-ht. of column for gap all around					
Length. (mm)	of column for no gap (mm)		Min. Lateral Displacement	Max. Lateral Displacement				
140	37.95	1	21.71	21.71				
	37.93	2	19.41	19.41				
160	17.32	1	16.91	16.91				
	17.32	2	17.12	17.12				
180	14.41	1	16.91	16.91				
	14.41	2	14.41	14.41				
200	19.30	1	18.52	18.52				
	19.30	2	16.91	16.91				

Table-3. Lateral displacement of Square CFST column with and without Gap

between steel tube and concrete core, the ultimate load-carrying capacity of column decreases compared to reference section and the propagation of gap from 1mm to 2mm on all four sides monotonically reduces the strength of the column. Moreover, the reduction in strength increases with an increase in the gap between the concrete core and steel tube. For the CFST columns having 1 mm and 2 mm gaps on all four sides, the maximum reduction in strength is observed as 3.3% and 3.2%, respectively, compared to reference section. The

reduction in strength of columns with gaps is less owing to lack of bonding between the steel tube and concrete due to the gap; as a result, the CFST column exhibit poor composite action.

7. Influence of Gap on Axial Load-Deformation Response of CFST Columns

The axial load-deformation response of CFST columns plays a vital role in understanding its inherent ductile behavior. To investigate the effect of the gap between steel tube and concrete core on the post-peak response of axial load-axial strain behavior of square section CFST columns, the axial load vs. axial-strain curves are plotted in Fig.9. The load-deformation response is plotted for 540 mm long CFST columns of square sections of side length varying between

140 mm to 200 mm at an interval of 20 mm having 1 mm and 2 mm gaps on all four sides. Their response is compared with a column of the same size but without the gap. It may be observed from the Fig.9. That, though, due to the gaps ultimate load is reduced, the post-peak axial load-deformation response of the CFST columns with various gaps is close to those having no-gap. This is due to the fact that as the axial load on column increases, concrete expands in a lateral direction due to Poisson's ratio. Once the gap between the steel tube and concrete core is filled, the concrete core comes in contact with a steel tube and develops composite action.

8. Influence of gap on Deformed Shape of CFST columns

In order to investigate the effect of the gap on the failure mode of CFST columns, the deformed shapes of CFST columns are examined. The deformed shapes for a typical column (140 mm size and 1&2 mm gap) for no-gap case together with for gaps on all four sides are shown in Fig 8.

The magnitudes of lateral displacements at mid-height of the column for all the cross-sections associated with different gap configurations are summarized in table 3. It may

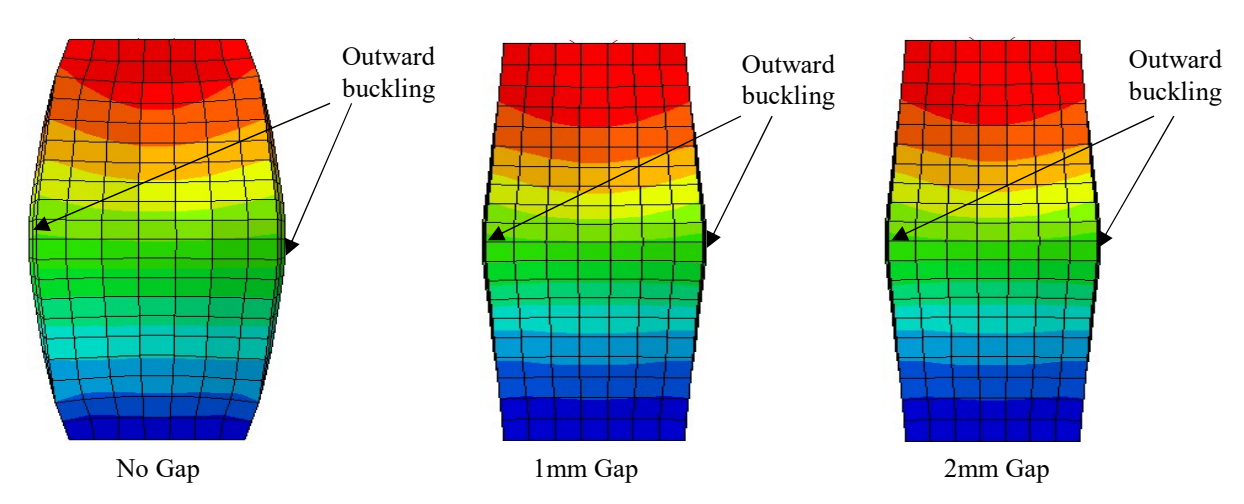


Fig.8 Influence of Gap on Deformed shape CFST columns at failure

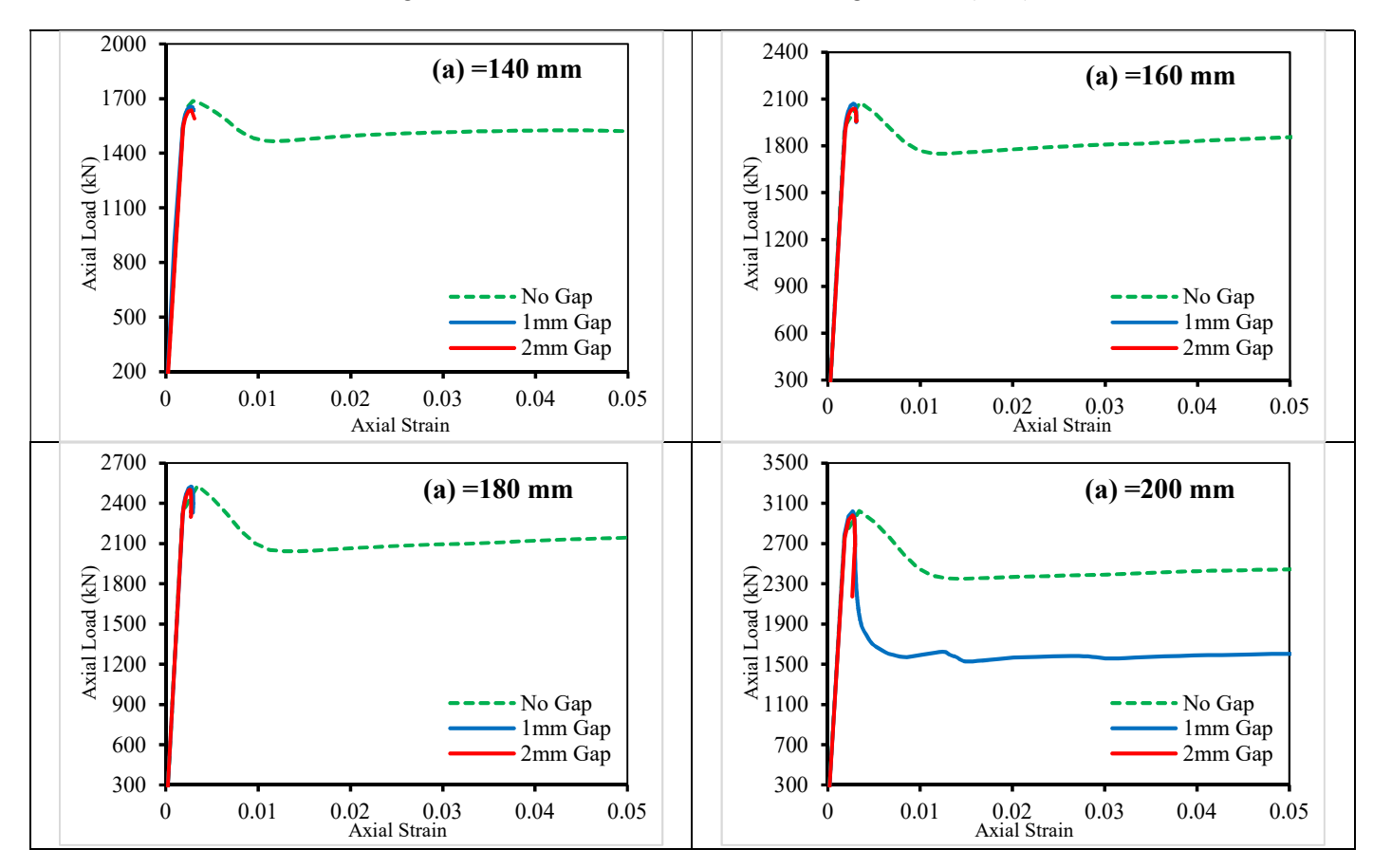


Fig. 9 Effect of gap on Axial Load-Deformation of CFST column of Different Cross-sections

be observed from the Table.3. that for the CFST columns with no-gap, the magnitudes of maximum and minimum lateral displacements at mid-height are equal and, consequently, no differential buckling occurs in this case as shown in Fig.10. Moreover, the table.3. indicates that while increasing the size of the column from 140 mm to 180 mm, the magnitudes of maximum, as well as minimum lateral displacements, decrease. However, for the size greater than 180 mm, they increase. Moreover, the table indicates that the smaller side length columns with the gaps are more prone to buckling, and the buckling decreases with an increase in the size of the column

9. Comparison of FEA Results with Euro Code Standards

The design provisions of Eurocode EC4 are used to compare the load-carrying capacity of the CFST columns under concentric load. The Eurocode-IV (EC4) presents expression to predict the load capacity of concrete-filled tubular columns, wherein the axial load carrying capacity is calculated as the sum of the axial strength contributions of concrete and steel together with the confinement effect if any. In the EC4 code, the confinement effect is considered for circular steel tubes only, and no confinement effect is considered for rectangular and square sections [24]. Schneider [17] and Hu [4] performed the tests on square section concrete-filled tubes and concluded that the

confinement effect provided by the square steel tube increases the ductility of the concrete core. Still, there was no significant improvement in the ultimate strength of CFST columns having depth-to-thickness ratios greater than 30 [15]. The lack of confinement effect in square section columns, especially for the high depth-to-thickness ratio, is due to local buckling of sidewalls. Therefore, while calculating the capacity of square section CFST columns, according to EC4, the confinement effect is neglected.

Moreover, in order to include the gap between the steel tube and concrete core, actual dimensions of the core have been considered for calculating the area of cross-section and moment of inertia of concrete core. The calculations for load carrying capacity for the square section column for a typical section (160 mm with a 2 mm gap on all four sides) are shown in the Appendix of this paper. The ultimate load-carrying capacities of square CFST columns with different sectional safely to design the square section columns even with the details determined using numerical simulation are compared with those calculated according to EC4[24]. It may be observed from Table.4 that the presence of a gap between steel tube and concrete core decreases the axial carrying capacity; however, for a given gap magnitude, on all four sides with gaps increases, the axial load carrying capacity decreases. Further, it may be noticed from the Table.4 that for CFST square section columns with no-gap, the EC4 underestimates the strength of more than 3.3% compared to numerically simulated strength. It is important to note for both the gap configurations considered, the strengths on numerical simulation, which infers that EC4 may be used

10. Conclusion

In order to validate the finite element modeling, the strength of a circular and square section CFSTs subjected to axial compressive load has been compared with the experimental data and the results found in good agreement. Further to check capability, the finite element simulation used in the present study in predicting the axial load carrying capacity of CFST with gaps, the axial load carrying capacity of circular sections containing gaps between steel tube and the concrete core was determined using the numerical simulation and found close to experimental data. Based on the study made to examine the effect of gaps between concrete core and steel tube on the structural response of CFST columns, the following conclusions have been drawn:

- The axial load carrying capacity of square section CFST columns monotonically reduces with an increase of size of gaps from 1mm to 2mm. Due to gaps between concrete core and steel tube, the maximum 3.3% reduction in strength was found in 140 mm side square CFST column having a 2 mm gap on all four sides.
- For all the sizes considered in this study, ultimate strength was found to decrease with increase in the gap from 1 mm to 2 mm and the maximum effect of an enhanced gap was found in 140 mm square side section CFST column with the gaps on all four sides where the strength decreased by 1.8% due to increase in the gap from 1 mm to 2 mm.
- Due to the gaps between concrete core and steel tube, though the noticeable reduction in ultimate load carrying capacity is found, the post-peak axial loaddeformation response of the CFST columns remains similar to that for the CFST column of the similar section having no gap.
- Smaller sizes of the columns with the gaps are more prone to the buckling, and the buckling decreases with an increase in size of the column.
- According to the Eurocode-4, the prediction of the ultimate load-carrying capacity of the Square CFST column has been found with a maximum difference of increase in 1.8% and a decrease of 3.2% compared to the FEM result.

Disclosures

Free Access to this article is sponsored by SARL ALPHA CRISTO INDUSTRIAL.

References

- Xiao Y, He W, Choi KK. Confined concrete-filled tubular columns. Journal of Structural Engineering 2005;131:488–97. https://doi.org/10.1061/(ASCE)0733-9445(2005)131:3(488).
- Sakino K, Nakahara H, Morino S, Nishiyama I. Behavior of centrally loaded concrete-filled steel-tube short columns. Journal of Structural Engineering 2004;130:180–8. https://doi.org/10.1061/(ASCE)0733-9445(2004)130:2(180).

- 3. Ronagh M and, Hu HTHTS, Huang CS, Wu MH, Wu YFYM, Xiao C, et al. Experimental studies on the behavior of concrete-filled steel tubes incorporating crumb rubber. Journal of Constructional Steel Research 2011;130:1–13. https://doi.org/10.1016/j.jcsr.2016.03.022.
- Hu HT, Huang CS, Wu MH, Wu YM. Nonlinear analysis of axially loaded concrete-filled tube columns with confinement effect. Journal of Structural Engineering 2003;129:1322–9. https://doi.org/10.1061/(ASCE)0733-9445(2003)129:10(1322).
- Aire C, Gettu R, Casas JR. Axially loaded concrete-filled steel tubes. Structural Concrete and Time - Proceedings of the Fib Symposium 2005;2:777-84.
- Xue JQ, Briseghella B, Chen BC. Effects of debonding on circular CFST stub columns. Journal of Constructional Steel Research 2012;69:64

 –76. https://doi.org/10.1016/j.jcsr.2011.08.002.
- Karthik MM, Mander JB. Stress-block parameters for unconfined and confined concrete based on a unified stress-strain model. Journal of Structural Engineering 2011;137:270–3. https://doi.org/10.1061/(ASCE)ST.1943-541X.0000294
- Liao FY, Han LH, Tao Z. Behaviour of CFST stub columns with initial concrete imperfection: Analysis and calculations. Thin-Walled Structures 2013;70:57–69. https://doi.org/10.1016/j.tws.2013.04.012.
- Tao Z, Song TY, Uy B, Han LH. Bond behavior in concrete-filled steel tubes. Journal of Constructional Steel Research 2016;120:81–93. https://doi.org/10.1016/j.jcsr.2015.12.030.
- Susantha KAS, Ge H, Usami T. Uniaxial stress-strain relationship of concrete confined by various shaped steel tubes. Engineering Structures 2001;23:1331–47. https://doi.org/10.1016/S0141-0296(01)00020-7.
- 11. Liao FY, Han LH, He SH. Behavior of CFST short column and beam with initial concrete imperfection: Experiments. Journal of Constructional Steel Research 2011;67:1922–35. https://doi.org/10.1016/j.jcsr.2011.06.009.
- ABAQUS (2014). Analysis user's manual 6.14-EF, Dassault Systems Simulia Corp., Providence, RI.
- 13. Kibriya T. Performance of Short CFST Columns using SCC with Blended Cement 2006:1–4.
- Xu B, Luan L, Chen H, Wang J, Zheng W. Experimental study on active interface debonding detection for rectangular concrete-filled steel tubes with surface wave measurement. Sensors (Switzerland) 2019;19. https://doi.org/10.3390/s19153248.
- Han LH, Yao GH, Tao Z. Performance of concrete-filled thin-walled steel tubes under pure torsion. Thin-Walled Structures 2007;45:24

 –36. https://doi.org/10.1016/j.tws.2007.01.008
- Han L-H, Zhao X-L, Tao Z. Tests and mechanics model for concretefilled SHS stub columns, columns and beam-columns. Steel and Composite Structures 2001;1:51–74. https://doi.org/10.12989/scs.2001.1.1.051.
- Schneider SP. Axially loaded concrete-filled steel tubes. JStruct Eng 1998;10:1125–1138.
- Han LH, Ye Y, Liao FY. Effects of Core Concrete Initial Imperfection on Performance of Eccentrically Loaded CFST Columns. Journal of Structural Engineering (United States) 2016;142:1–13. https://doi.org/10.1061/(ASCE)ST.1943-541X.0001604.
- Han LH, Yao GH, Zhao XL. Tests and calculations for hollow structural steel (HSS) stub columns filled with self-consolidating concrete (SCC). Journal of Constructional Steel Research 2005;61:1241–69. https://doi.org/10.1016/j.jcsr.2005.01.004.
- Lee E, Yun BH, Shim HJ, Chang KH, Lee GC. Torsional Behavior of Concrete-Filled Circular Steel Tube Columns 2009;135:1250–8.
- Li P, Zhang T, Wang C. Behavior of Concrete-Filled Steel Tube Columns Subjected to Axial Compression. Advances in Materials

- Science and Engineering 2018;2018. https://doi.org/10.1155/2018/4059675
- Lu ZH, Zhao YG. Mechanical Behavior and Ultimate Strength of Circular Cft Columns Subjected To Axial Compression Loads. The 14th World Conference on Earthquake Engineering 2008.
- Attard MM, Setunge S. Stress-strain relationship of confined and unconfined concrete. ACI Materials Journal 1996;93:432–42. https://doi.org/10.14359/9847.
- 24. EN 1994-1-1:2004. Design of composite steel and concrete structures, Part 1- 1:General rules and rules for buildings. EUROCODE 4, European Committee for Standardization, 2004.
- Bardet JP. Lode dependences for isotropic pressure-sensitive elastoplastic materials. Journal of Applied Mechanics, Transactions ASME 1990;57:498. https://doi.org/10.1115/1.2897051
- Maïolino S, Luong MP. Measuring discrepancies between Coulomb and other geotechnical criteria: Drucker-Prager and Matsuoka-Nakai. 7th Euromech Solid Mechanics Conference (ESMC2009), Lisbon 2009.
- Wai-Fah Chen. Plasticity in reinforced concrete. New York: McGraw-Hill: 1982.
- By Feng-Bao Lin1 and Zdenek P. Bazant 2 F. CONVEXITY OF SMOOTH YIELD SURFACE OF FRICTIONAL MATERIAL. Journal of Engineering Mechanics 1986;112:1259–62.

- Masad E, Dessouky S, Little D. Development of an elastoviscoplastic microstructural-based continuum model to predict permanent deformation in hot mix asphalt. International Journal of Geomechanics 2007;7:119–30. https://doi.org/10.1061/(ASCE)1532-3641(2007)7:2(119).
- 30. Tao Z, Wang Z Bin, Yu Q. Finite element modelling of concrete-filled steel stub columns under axial compression. Journal of Constructional Steel Research 2013;89:121–31. https://doi.org/10.1016/j.jcsr.2013.07.001.
- 31. Tao Z, Wang Z Bin, Yu Q. Finite element modelling of concrete-filled steel stub columns under axial compression. Journal of Constructional Steel Research 2013;89:121–31. https://doi.org/10.1016/j.jcsr.2013.07.001.
- Liao FY, Han LH, Tao Z, Rasmussen KJR. Experimental Behavior of Concrete-Filled Stainless Steel Tubular Columns under Cyclic Lateral Loading. Journal of Structural Engineering (United States) 2017;143:1– 15. https://doi.org/10.1061/(ASCE)ST.1943-541X.0001705.
- Lai MH, Ho JCM. A theoretical axial stress-strain model for circular concrete-filled-steel-tube columns. Engineering Structures 2016. https://doi.org/10.1016/j.engstruct.2016.06.048.